

# Systematic Effect of Benzo-Annellation on Oxo–Hydroxy Tautomerism of Heterocyclic Compounds. Experimental Matrix-Isolation and Theoretical Study

Anna Gerega,<sup>†</sup> Leszek Lapinski,<sup>†</sup> Maciej J. Nowak,<sup>\*,†</sup> Al'ona Furmanchuk,<sup>‡</sup> and Jerzy Leszczynski<sup>‡</sup>

*Institute of Physics, Polish Academy of Sciences, Al. Lotnikow 32/46, 02-668 Warsaw, Poland, and Computational Center for Molecular Structure and Interactions, Department of Chemistry, Jackson State University, Jackson, Mississippi 39217*

*Received: January 17, 2007; In Final Form: March 5, 2007*

Oxo–hydroxy tautomerism and phototautomerism of 2-quinolinone, 1-isoquinolinone, 3-hydroxyisoquinoline, 2-quinoxalinone, and 4-quinazolinone were studied using the matrix-isolation technique. These compounds contain a benzene ring fused with a heterocyclic ring of 2-pyridinone, 2-pyrazinone, or 4-pyrimidinone. It turned out that direct attachment of a benzene ring to a heterocycle leads to a very pronounced increase of the relative stability of oxo tautomers (in comparison with the tautomerism of the parent compounds 2-pyridinone, 2-pyrazinone, and 4-pyrimidinone). The only exception concerns 3-hydroxyisoquinoline, where fusion with a benzene ring enforces rearrangement of the double- and single-bond system in the oxo tautomer. This destabilizes substantially the oxo form with respect to the hydroxy tautomer. The ratios of population of the oxo and hydroxy tautomers observed in Ar matrixes correspond to the tautomeric equilibria of the compounds in the gas phase. These equilibria were well reproduced by theoretical calculations carried out at the QCISD and QCISD(T) levels. The combined experimental and theoretical results reveal links between aromaticity and tautomerism. Moreover, a UV-induced phototautomeric reaction transforming the oxo forms into the hydroxy tautomers was observed for all (except 3-hydroxyisoquinoline) studied compounds. This photoeffect allowed separation of the IR spectra of the tautomers in question.

## Introduction

Prototropic tautomerism, a particular case of isomerism, plays an important role in modern organic chemistry, biochemistry, medicinal chemistry, and molecular biology. It has been suggested that the oxo–hydroxy tautomerization process in heterocyclic compounds might be at the origin of genetic mutations.<sup>1–3</sup>

2-Quinolinone (carbostyril) can exist in two forms, referred to as the oxo **2QLo** and hydroxy **2QLh** tautomers (Chart 1). These two forms may interconvert by H-atom transfer between the oxygen atom and the nitrogen atom of the pyridine ring. The electronic properties and absorption spectra of the tautomers of 2-quinolinone have been investigated by several authors.<sup>4–7</sup> These studies refer to the widely cited gas calorimetric measurement results,<sup>4</sup> which claim that the hydroxy **2QLh** form of gaseous 2-quinolinone is lower in energy (by 1.2 kJ mol<sup>-1</sup>) than the oxo **2QLo** tautomer of the compound. In the present work we demonstrate that the data reported by Beak<sup>4</sup> are not correct.

In the experiments on 2-quinolinone molecules in seeded supersonic jet expansions,<sup>5</sup> the observed spectra of dispersed fluorescence (DF) and of fluorescence excitation (FE) were more intense for the hydroxy tautomer **2QLh** than for the oxo form **2QLo**. This observation might suggest that (in agreement with Beak's report)<sup>4</sup> the population of the **2QLh** tautomer in the gas phase is greater than the population of **2QLo**. However, the transition moments between S<sub>0</sub> and S<sub>1</sub> states can be very

different for both tautomers in question, and conclusion about relative populations of the tautomers on the basis of DF and FE spectra can be misleading.

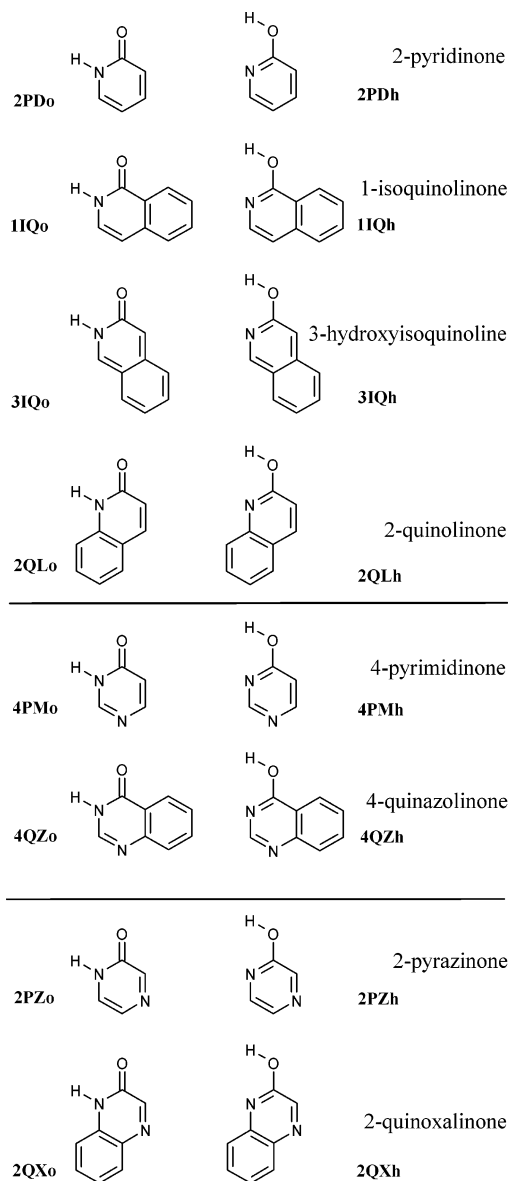
Much more information is available about the tautomerization of 2(1H)-pyridinone (**2PDo**) ↔ 2-hydroxypyridine (**2PDh**), since tautomerism of this system represents a model for intramolecular proton transfer in a heterocyclic molecule. The energy difference ( $\Delta E$ ) between **2PDo** and **2PDh** forms (see Chart 1) of this compound in the gas phase was experimentally determined in a reliable way. Hatherley et al.<sup>8</sup> investigated the tautomerism of the **2PDo** ↔ **2PDh** system by microwave spectroscopy. On the basis of relative intensities of the observed microwave absorption bands and using the measured values of the dipole moments, these authors estimated the energy difference between the vibrational ground states of the two (hydroxy and oxo) tautomers to be  $\Delta E = -3.2$  kJ mol<sup>-1</sup>, in favor of the hydroxy form. Earlier, the results of infrared investigation of gaseous **2PD** at variable temperature were reported by Nowak et al.<sup>9</sup> In that work  $\Delta E$  was estimated to be equal  $-3.0 \pm 0.6$  kJ mol<sup>-1</sup>. This value is in good agreement with the results obtained by Hatherley et al.<sup>8</sup>

Many attempts to theoretically reproduce the experimental  $\Delta E$  value were made using different methods of quantum chemistry.<sup>10–13</sup> The relative energies of the tautomers of 2-pyridinone were studied by a variety of quantum chemical methods,<sup>14</sup> among them density functional theory (DFT), the ab initio Hartree–Fock (HF) methods, standard second-order Møller–Plesset perturbation theory (MP2), an improved version of it (SCS-MP2), coupled-cluster (CCSD) and the very similar quadratic configuration interaction including single and double excitations (QCISD), and perturbative corrections for triple

\* To whom correspondence should be addressed. E-mail: mjnnow@ifpan.edu.pl.

<sup>†</sup> Polish Academy of Sciences.

<sup>‡</sup> Jackson State University.

**CHART 1: Structures of the Studied Compounds and Abbreviations Used**

excitations [QCISD(T)]. The accumulated theoretical data clearly show that the popular DFT and MP2 methods are not able to correctly reproduce the experimentally measured difference of energies of the tautomers. As pointed out by Piacenza and Grimme,<sup>14</sup> the DFT methods (using different exchange-correlation functionals) underestimate the stability due to the aromatic character of the heterocyclic ring of the hydroxy tautomer. Hence, these methods predict that the oxo tautomer of **2PD** is more stable than the hydroxy form. This does not agree with an energetic order of **2PD<sub>o</sub>** and **2PD<sub>h</sub>** deduced from experimental investigations. The MP2 method predicts correctly that the hydroxy form of the compound should be more stable, but the MP2-calculated energy difference (ca.  $-12 \text{ kJ mol}^{-1}$ ) is significantly overestimated. The calculations carried out within the current work (presented in Table 1) fully support these conclusions.

More encouraging are the results of the theoretical predictions of the relative energies of the **2PD<sub>h</sub>** and **2PD<sub>o</sub>** forms obtained by using the QCISD and QCISD(T) methods. The calculations carried out at these levels [previously by Piacenza and Grimme,<sup>14</sup> and in the current work (Table 1)] yielded good approximations

to the experimentally measured value of  $\Delta E \approx -3 \text{ kJ mol}^{-1}$ . One of the aims of the present work is to assess if these methods [QCISD and QCISD(T)] would predict accurately the energy differences also for other heterocyclic systems.

Two types of intramolecular proton transfer processes induced by excitation to electronic states higher than  $S_0$  are known. One of them is the excited state intramolecular proton transfer (ESIPT).<sup>15–18</sup> In the work on carbostyryl in supersonic jet expansion Nimlos et al.<sup>5</sup> were searching for the ESIPT process, which would transform the hydroxy form of the compound into the oxo tautomer. However, no spectral indications of occurrence of a photoprocess of this type were found. On the other hand, UV-induced intramolecular proton transfer converting the oxo forms of 2-pyridinone (**2PD**) or 4-pyrimidinone (**4PM**) into the corresponding hydroxy tautomers was observed<sup>9,19–22</sup> for monomers of these compounds isolated in low-temperature Ar matrixes. In these processes the electronically excited oxo tautomer of a compound converts to the hydroxy form during relaxation to the ground state. Such phototautomeric transformations are of a quite different nature from those of the well-studied ESIPT type.

In the present work, tautomerism and phototautomerism of 2-quinolinone (**2QL**, carbostyryl), 1-isoquinolinone (**1IQ**, isocarbostyryl), 3-hydroxyisoquinoline (**3IQ**), 2-quinoxalinone (**2QX**), and 4-quinazolinone (**4QZ**; see Chart 1) were studied using the matrix-isolation technique. For each of these compounds, the ratio of oxo and hydroxy tautomers trapped from the gas phase into a low-temperature matrix was compared with the results of theoretical predictions of the relative energies of the oxo and hydroxy tautomeric forms. The experimental and theoretical results obtained for the compounds listed above are juxtaposed with the tautomeric equilibria observed for 2-pyridinone (**2PD**), 4-pyrimidinone (**4PM**), and 2-pyrazinone (**2PZ**), which served as model systems with only one six-membered ring per molecule. This comparison allowed us to conclude about the influence of a directly attached benzene ring on tautomerism of systems, for which 2-pyridinone is an archetype.

**Experimental Section**

2-Pyridinone, 4-pyrimidinone, 2-quinolinone, 1-isoquinolinone, 3-hydroxyisoquinoline, 2-quinoxalinone, and 4-quinazolinone used in the present study were commercial products supplied by Sigma-Aldrich. The sample of 2-pyrazinone was synthesized using the procedure described in refs 23–25. To prepare a low-temperature matrix, a solid sample of a studied compound was electrically heated in a miniature glass oven placed in the vacuum chamber of a continuous-flow helium cryostat. The vapors of the compound were deposited, together with a large excess of argon, on a CsI window cooled to 10 K. In order to deposit monomeric matrixes, the appropriate vapor pressure over a solid compound was obtained at the oven temperatures of 340 K for **2PD**, 400 K for **4PM**, 360 K for **2PZ**, 450 for **2QL**, 450 for **2QX**, 420 K for **1IQ**, 470 K for **4QZ**, and 420 K for **3HQ**. The argon matrix gas of spectral purity 6.0 was supplied by Linde AG. The IR spectra were recorded with  $0.5 \text{ cm}^{-1}$  resolution using a Thermo Nicolet Nexus 670 FTIR spectrometer equipped with a KBr beam splitter and a DTGS detector. Matrixes were irradiated with light from a HBO200 high-pressure mercury lamp fitted with a water filter and an appropriate cutoff filter transmitting light with  $\lambda > 300 \text{ nm}$ ,  $\lambda > 320 \text{ nm}$ , or  $\lambda > 335 \text{ nm}$ .

**Computational Section**

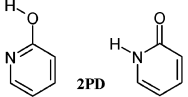
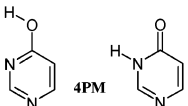
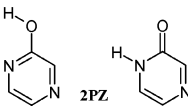
The structures of all species considered in the current work are presented in Chart 1. The geometries of these forms were

**TABLE 1: Calculated Electronic Energy Difference  $\Delta E_{el} = \Delta E_{el}(\text{hydroxy}) - \Delta E_{el}(\text{oxo})$ , Internal Energy Difference  $\Delta E = \Delta E(\text{hydroxy}) - \Delta E(\text{oxo})$ , and Free Helmholtz Energy Difference  $\Delta F = \Delta F(\text{hydroxy}) - \Delta F(\text{oxo})$  between the Hydroxy and Oxo Tautomers of 2(1H)-Pyridinone/2-Hydroxypyridine (kJ mol<sup>-1</sup>)**

method	$\Delta E_{el}$	$\Delta E = \Delta H^a$ (at 340 K)	$\Delta F = \Delta G^a$ (at 340 K)
B3LYP/cc-pVTZ//B3LYP/cc-pVTZ	2.52	1.83	2.40
MP2/cc-pVDZ//MP2/cc-pVDZ	-10.70	-11.20	-10.54
MP2/cc-pVTZ//MP2/cc-pVTZ	-11.76	-12.26	-11.72
MP2/cc-pVDZ//B3LYP/cc-pVTZ	-10.44	-11.13	-10.56
MP2/cc-pVTZ//B3LYP/cc-pVTZ	-11.82	-12.51	-11.94
CCSD(T)/cc-pVDZ//B3LYP/cc-pVTZ	-5.76	-6.45	-5.88
CCSD(T)/cc-pVTZ//B3LYP/cc-pVTZ	-6.48	-7.17	-6.60
QCISD/cc-pVDZ//B3LYP/cc-pVTZ	-2.50	-3.19	-2.62
QCISD/cc-pVTZ//B3LYP/cc-pVTZ	-3.32	-4.01	-3.44
QCISD(T)/cc-pVDZ//B3LYP/cc-pVTZ	-4.79	-5.48	-4.91
QCISD(T)/cc-pVTZ//B3LYP/cc-pVTZ	-5.49	-6.18	-5.61
experiment	$-2.5 \pm 0.6^b$	$-3.0 \pm 0.6^b$	$-2.9 \pm 0.5^c$

<sup>a</sup> Vibrational and rotational contributions to the theoretical values of  $\Delta E$  and  $\Delta F$  were calculated at the DFT(B3LYP)/cc-pVTZ level, except for calculations carried out at the MP2/cc-pVDZ//MP2/cc-pVDZ and MP2/cc-pVTZ//MP2/cc-pVTZ levels where vibrational and rotational contributions were calculated using MP2/cc-pVDZ//MP2/cc-pVDZ and MP2/cc-pVTZ//MP2/cc-pVTZ methods, respectively. <sup>b</sup> The value of  $\Delta E_{el}$  was estimated by subtraction from the experimentally measured  $\Delta E^{8,9}$  the  $\Delta(\text{ZPE}) = -0.54$  kJ mol<sup>-1</sup> value calculated at the DFT(B3LYP)/cc-pVTZ level. <sup>c</sup> The value of  $\Delta F$  was experimentally estimated on the basis of the ratio of oxo and hydroxy tautomers trapped from the gas phase (at 340 K) into a low-temperature Ar matrix.<sup>9</sup>

**TABLE 2: Experimental and Theoretically Calculated Free Energy Differences between the Hydroxy and Oxo Tautomers of 2-Pyridinone, 4-Pyrimidinone, and 2-Pyrazinone**

compounds	$\Delta E_{el}^a$	$\Delta F = \Delta G^b$ at T	$\Delta F_{\text{exp}} = \Delta G_{\text{exp}}$ at T	T	Experimental ratio of hydroxy and oxo forms (at T)
	kJ mol <sup>-1</sup>	kJ mol <sup>-1</sup>	kJ mol <sup>-1</sup>	Kelvin	[hydroxy]:[oxo]
 2PD	-2.50 (-4.79)	-2.62 (-4.91)	$-2.9 \pm 0.5$	340	2.8 : 1
 4PM	4.02 (2.09)	4.19 (2.26)	$2.4 \pm 0.3$	400	1 : 2.1
 2PZ	-5.26 (-6.78)	-5.19 (-6.71)	$-8.0 \pm 1.0$	360	14 : 1

<sup>a</sup>  $\Delta E_{el}$  difference of electronic energies ( $E_{\text{hydroxy}} - E_{\text{oxo}}$ ) calculated at the QCISD/cc-pVDZ or QCISD(T)/cc-pVDZ (given in parentheses) levels at geometry optimized using the DFT(B3LYP)/cc-pVTZ method. <sup>b</sup>  $\Delta F = \Delta G$  difference of free Helmholtz = free Gibbs energies ( $F_{\text{hydroxy}} - F_{\text{oxo}}$ ) calculated using the  $\Delta E_{el}$  values and thermal and entropy corrections obtained on the basis of the DFT(B3LYP)/cc-pVTZ computed vibrational frequencies and rotational constants.

optimized using the hybrid Hartree–Fock and density functional theory method DFT(B3LYP) with the Becke’s three-parameter exchange functional<sup>26</sup> and gradient-corrected functional of Lee, Yang, and Parr.<sup>27,28</sup> Dunning’s correlation-consistent basis set of triple- $\zeta$  quality with polarization functions on all atoms (cc-pVTZ)<sup>29</sup> was used in these calculations. Using the reference optimized geometries, the harmonic vibrational frequencies and IR intensities were calculated. The nature of the stationary points has been determined by analysis of the computed Hessian matrices. All the optimized geometries correspond to minima on the potential energy surfaces. Finally, at the DFT(B3LYP)/cc-pVTZ optimized geometries, single-point calculations of electronic energies ( $E_{el}$ ) were carried out using the quadratic configuration interaction method<sup>30</sup> with single and double excitations (QCISD) and perturbative corrections for triple excitations [QCISD(T)]. In order to compute the Gibbs free energy differences between the hydroxy and oxo tautomers, the relative electronic energies were corrected for thermal and entropy terms using the harmonic oscillator and rigid rotor approximations. The temperature parameter used in these

calculations was equal to the temperature of evaporation of a compound during matrix deposition. For a tautomerization reaction, the  $\Delta pV$  and  $p\Delta V$  terms equal zero, hence the Gibbs free energy difference between tautomers ( $\Delta G$ ) equals the Helmholtz free energy difference ( $\Delta F$ ). The results of the  $\Delta E_{el}$  and  $\Delta G = \Delta F$  calculations are presented in Tables 1–5. For the 2(1H)-pyridinone–2-hydroxypyridine system (Table 1),  $\Delta E_{el}$  was also calculated using the second order of the Møller–Plesset perturbation theory (MP2)<sup>31</sup> as well as using the coupled-cluster method<sup>32,33</sup> with single, double, and noniterative triple excitations [CCSD(T)]. Both cc-pVDZ and cc-pVTZ basis sets were utilized in these calculations. The MP2 energy calculations were performed not only at the DFT(B3LYP) optimized geometry, but also at geometry optimized at the MP2 level (see Table 1). All the calculations in the current work were carried out using the Gaussian 03 program.<sup>34</sup>

## Results and Discussion

**Systems with Single Heterocyclic Rings.** A significant amount of computational effort (see the Introduction) has been

devoted so far to theoretical prediction of the tautomeric equilibrium in  $2\text{PD}_{\text{o}} \leftrightarrow 2\text{PD}_{\text{h}}$ . Although a nice reproduction of experimental data has been achieved when calculations were performed at QCISD or QCISD(T) levels, it was not tested if this agreement was accidental, happening just for the case of the  $2\text{PD}$  system. Hence, it was desirable to carry out analogous calculations also for other tautomerizing heterocyclic compounds and to compare the results of such calculations with experimental measurements.

Whereas for  $2\text{PD}$  the hydroxy tautomer is more stable and in the gas phase the ratio of the hydroxy and oxo forms equals<sup>9</sup> (approximately) 2.8:1, the tautomeric equilibrium is somewhat different for two related heterocycles:  $4\text{PM}_{\text{o}} \leftrightarrow 4\text{PM}_{\text{h}}$  and  $2\text{PZ}_{\text{o}} \leftrightarrow 2\text{PZ}_{\text{h}}$  (Table 2). For the first compound ( $4\text{PM}$ ), the oxo form is more stable than the hydroxy tautomer and the two forms appear in the gas phase with the ratio [hydroxy]:[oxo] equal to (approximately) 1:2. For the latter compound ( $2\text{PZ}$ ), the dominance of the hydroxy tautomer is significantly more pronounced ([hydroxy]:[oxo]  $\cong$  14:1) than it was the case for  $2\text{PD}_{\text{o}} \leftrightarrow 2\text{PD}_{\text{h}}$ . That is why these two species were good candidates for tests of the performance of the QCISD and QCISD(T) methods.

The results of the QCISD and QCISD(T) calculations (presented in Table 2) show that these methods correctly predict the increase of the relative stability of the oxo tautomer of  $4\text{PM}$  in comparison to the tautomeric equilibrium in  $2\text{PD}$ . Also, the increase of the relative stability of the hydroxy tautomer of  $2\text{PZ}$  (with respect to the corresponding values obtained for  $2\text{PD}$ ) was well predicted at QCISD and QCISD(T) levels. Not only shifts of tautomeric equilibria of  $4\text{PM}_{\text{o}} \leftrightarrow 4\text{PM}_{\text{h}}$  and  $2\text{PZ}_{\text{o}} \leftrightarrow 2\text{PZ}_{\text{h}}$  with respect to the equilibrium in  $2\text{PD}_{\text{o}} \leftrightarrow 2\text{PD}_{\text{h}}$ , but also the absolute values of the computed energy differences between the oxo and hydroxy tautomers are in fair agreement with experiment, for all three systems. These results show that the QCISD and QCISD(T) methods are able to provide reliable relative energies of tautomers for the particular case of  $2\text{PD}_{\text{o}} \leftrightarrow 2\text{PD}_{\text{h}}$  as well as for other heterocyclic compounds.

In the following section the QCISD and QCISD(T) methods will be used to predict gas-phase equilibria for a series of compounds:  $2\text{QL}$ ,  $1\text{IQ}$ ,  $3\text{IQ}$ ,  $4\text{QZ}$ , and  $2\text{QX}$ . These compounds are analogous to those considered above, but with a benzene ring directly attached to a heterocyclic six-membered ring. The results of such calculations will be compared with the experimental observations of the gas-phase equilibrium of tautomers trapped in low-temperature matrices. To the best of our knowledge, no report on reliable experimental or theoretical studies of tautomerism of these systems is available to date.

#### Systems with Fused Heterocyclic and Benzene Rings.

*2-Quinoxalinone*, *2-Quinolinone*, *1-Isoquinolinone*, and *4-Quinazolinone*. A mere glance at the relative intensities of the bands due to the stretching vibrations of the O–H group ( $2\text{QX}_{\text{h}}$  form) and the N–H group ( $2\text{QX}_{\text{o}}$  form) in the experimental IR spectrum of 2-quinoxalinone isolated in a low-temperature Ar matrix (Figure 1) strongly suggests that a vast majority of molecules of this compound adopt the oxo  $2\text{QX}_{\text{o}}$  form. The observation of a very low-intensity  $\nu(\text{OH})$  band (at  $3568\text{ cm}^{-1}$ ), alongside the much, much stronger  $\nu(\text{NH})$  band (at  $3419\text{ cm}^{-1}$ ), indicates also that a very small fraction of  $2\text{QX}$  molecules adopt the hydroxy  $2\text{QX}_{\text{h}}$  form. Other very weak bands due to the  $2\text{QX}_{\text{h}}$  tautomer were identified in the IR spectrum thanks to the effect of UV irradiation of the matrix. Upon such irradiation, the molecules in the oxo form converted into the hydroxy tautomer and the IR spectrum of this latter form increased many times (see Figure 2, see also next section

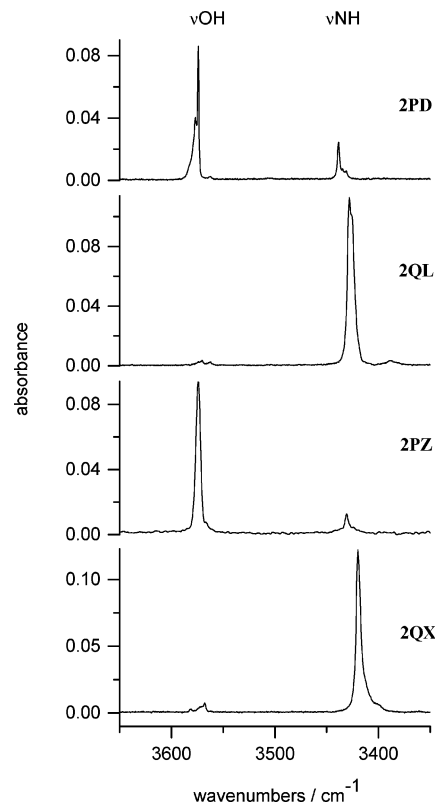


**Figure 1.** High-frequency regions of the infrared spectra of 2-pyridinone ( $2\text{PD}$ ), 2-quinolinone ( $2\text{QL}$ ), 2-pyrazinone ( $2\text{PZ}$ ), and 2-quinoxalinone ( $2\text{QX}$ ) isolated in Ar matrices. The IR bands present in this spectral range are due to  $\nu(\text{OH})$  and  $\nu(\text{NH})$  vibrations and are characteristic of the hydroxy and oxo tautomers, respectively.

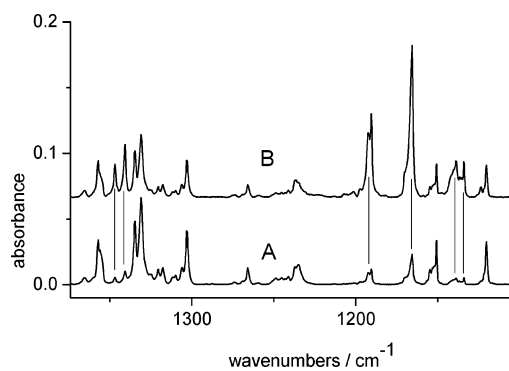


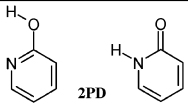
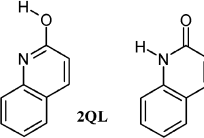
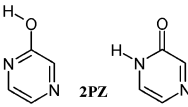
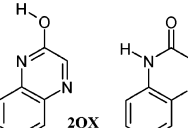
**Figure 2.** Fragment of the IR spectrum of 2-quinoxalinone ( $2\text{QX}$ ) isolated in an Ar matrix: (A) spectrum recorded after deposition of the matrix; (B) spectrum recorded after 6.5 h of UV ( $\lambda > 335\text{ nm}$ ) irradiation. Vertical lines indicate bands due to the hydroxy tautomer, which were present in spectrum A and grew after UV irradiation of the matrix.

where phototautomerism is described in more detail). Without this photoeffect, it would be very difficult to identify the bands due to the  $2\text{QX}_{\text{h}}$  tautomer in the initial IR spectrum of the compound. Having the observed IR bands assigned to either the oxo form or the hydroxy form, the ratio of the tautomers in the matrix was assessed using the formula

$$\frac{[\text{hydroxy}]}{[\text{oxo}]} = \frac{\sum I_{\text{hydroxy}}^{\text{exp}} / \sum A_{\text{hydroxy}}^{\text{theor}}}{\sum I_{\text{oxo}}^{\text{exp}} / \sum A_{\text{oxo}}^{\text{theor}}} \quad (1)$$

where  $\sum I_{\text{hydroxy}}^{\text{exp}}$  and  $\sum I_{\text{oxo}}^{\text{exp}}$  are sums of integrated intensities of the bands observed in the spectra of the hydroxy and oxo forms,

**TABLE 3: Experimental and Theoretically Calculated Free Energy Differences between the Hydroxy and Oxo Tautomers of 2-Pyridinone, 2-Quinolinone, 2-Pyrazinone, and 2-Quinoxalinone**

compounds	R(C-N) <sup>a</sup>	$\Delta E_{\text{el}}^b$	$\Delta F = \Delta G^c$ at T	$\Delta F_{\text{exp}} = \Delta G_{\text{exp}}$ at T	T	Experimental ratio of hydroxy and oxo forms (at T) [hydroxy]:[oxo]
	Å	kJ mol <sup>-1</sup>	kJ mol <sup>-1</sup>	kJ mol <sup>-1</sup>	Kelvin	
 <b>2PD</b>	1.408	-2.50 (-4.79)	-2.62 (-4.91)	$-2.9 \pm 0.5$	340	2.8 : 1
 <b>2QL</b>	1.393	15.65 (12.84)	15.70 (12.89)	$17 \pm 1.5$	450	1 : 95
 <b>2PZ</b>	1.400	-5.26 (-6.78)	-5.19 (-6.71)	$-8.0 \pm 1.0$	360	14 : 1
 <b>2QX</b>	1.382	14.43 (11.34)	14.65 (11.56)	$14 \pm 1.0$	450	1 : 40

<sup>a</sup> Distance between C and N atoms in the H–N–C=O fragment of the oxo tautomer. The value has been obtained by geometry optimization carried out at the DFT(B3LYP)/cc-pVTZ level. <sup>b</sup>  $\Delta E_{\text{el}}$  difference of electronic energies ( $E_{\text{hydroxy}} - E_{\text{oxo}}$ ) calculated at the QCISD/cc-pVDZ or QCISD(T)/cc-pVDZ (given in parentheses) levels at geometry optimized using the DFT(B3LYP)/cc-pVTZ method. <sup>c</sup>  $\Delta F = \Delta G$  difference of free Helmholtz = free Gibbs energies ( $F_{\text{hydroxy}} - F_{\text{oxo}}$ ) calculated using the  $\Delta E_{\text{el}}$  values and thermal and entropy corrections obtained on the basis of the DFT(B3LYP)/cc-pVTZ computed vibrational frequencies and rotational constants.

respectively;  $\sum A_{\text{hydroxy}}^{\text{theor}}$  and  $\sum A_{\text{oxo}}^{\text{theor}}$  are sums of absolute intensities of the corresponding bands calculated at the DFT(B3LYP)/cc-pVTZ level.

As a result, the ratio of the hydroxy and oxo forms of **2QX** in an Ar matrix was estimated to be equal to 1:40. The ratio of tautomers trapped in a low-temperature matrix is believed to be equal to the ratio of these forms in the gas phase from which the matrix was formed. This was demonstrated in one of the previous works<sup>9</sup> on 2-pyridinone, where tautomerism of the **2PDh** ↔ **2PDo** system was studied for the compound in the gas phase as well as for the compound isolated in low-temperature matrixes. Hence, on the basis of the ratio of the hydroxy and oxo forms isolated in an Ar matrix, the experimental difference of free energies of the two tautomers can be estimated using the formula

$$\Delta F_{\text{exp}} = F_{\text{hydroxy}} - F_{\text{oxo}} = -RT \ln \frac{[\text{hydroxy}]}{[\text{oxo}]} \quad (2)$$

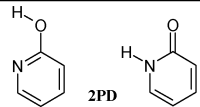
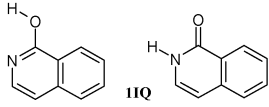
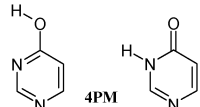
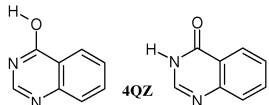
The result of such an assessment is presented in Table 3, where the  $\Delta F_{\text{exp}}$  value is compared with the results of theoretical predictions. As can be seen, the agreement between the experimental and theoretically predicted  $\Delta F$  values is quite satisfactory. Theory (at the QCISD level) and experimental estimations provide the value  $\Delta F \approx 14 \text{ kJ mol}^{-1}$ , in favor of the significantly more stable **2QXo** oxo tautomer.

The experimental observation of a strong dominance of the oxo form of **2QX** is in sharp contrast to the observations of tautomeric equilibrium in 2-pyrazinone (**2PZ**). For the latter compound, the dominating form is the hydroxy tautomer. Comparison of the [hydroxy]:[oxo] ratio in **2QX** (1:40) with the corresponding ratio for **2PZ** (14:1) shows the magnitude of

the difference in tautomeric equilibria in these two related compounds. This is illustrated by a substantial difference of relative intensities of the bands due to the  $\nu(\text{OH})$  and  $\nu(\text{NH})$  vibrations observed in the IR spectra recorded for both compounds isolated in Ar matrixes (see Figure 1). Such a sizable shift of tautomeric equilibrium, introduced by a direct attachment of benzene ring to the heterocyclic ring of **2PZ**, is also predicted theoretically. The results of theoretical and experimental estimations of the free energy difference between the hydroxy and oxo forms of **2PZ** are compared in Table 3 with the corresponding  $\Delta F$  values obtained for **2QX**.

Calculations carried out at QCISD or QCISD(T) levels predict the oxo form of carbostyryl (**2QL**) to be more stable than the hydroxy tautomer (see Table 3). At the QCISD level of theory the predicted value of the free energy difference between the **2QLh** and **2QLo** forms is as high as  $16 \text{ kJ mol}^{-1}$ . This value is even higher than  $\Delta F$  predicted (at the same theory level) for the 2-quinoxalinone (**2QX**) system (discussed in the paragraphs above). Similarly, the calculations carried out at the QCISD(T) level predict also a larger difference in stabilities of the hydroxy and oxo forms (in favor of the oxo tautomer) in the case of **2QL**, in comparison with the corresponding value obtained for **2QX** (Table 3). These predictions are in nice agreement with experimental observations. In the IR spectrum of **2QL** isolated in an Ar matrix, the bands indicating the presence of a very tiny amount of the hydroxy tautomer are barely detectable and the whole spectrum is dominated strongly by the bands due to the oxo form. In the high-frequency region of the spectrum of **2QL** monomers in an Ar matrix (Figure 1), the absorption at the usual position of a band due to  $\nu(\text{OH})$  vibration is extremely weak. Nevertheless, using methods similar to those applied for the case of **2QX**, it was possible to assess the relative

**TABLE 4: Experimental and Theoretically Calculated Free Energy Differences between the Hydroxy and Oxo Tautomers of 2-Pyridinone, 1-Isoquinolinone, 4-Pyrimidinone, and 4-Quinazolinone**

compounds	R(C-N) <sup>a</sup>	$\Delta E_{el}^b$	$\Delta F = \Delta G^c$ at T	$\Delta F_{exp} = \Delta G_{exp}$ at T	T	Experimental ratio of hydroxy and oxo forms (at T) [hydroxy]:[oxo]
	Å	kJ mol <sup>-1</sup>	kJ mol <sup>-1</sup>	kJ mol <sup>-1</sup>	Kelvin	
 <b>2PD</b>	1.408	-2.50 (-4.79)	-2.62 (-4.91)	-2.9 ± 0.5	340	2.8 : 1
 <b>1IQ</b>	1.391	23.97 (21.17)	23.68 (20.88)	>17	420	hydroxy form not observed
 <b>4PM</b>	1.415	4.02 (2.09)	4.19 (2.26)	2.4 ± 0.3	400	1 : 2.1
 <b>4QZ</b>	1.399	28.79 (25.77)	28.78 (25.76)	>17	470	hydroxy form not observed

<sup>a</sup> Distance between C and N atoms in the H–N–C=O fragment of the oxo tautomer. The value has been obtained by geometry optimization carried out at the DFT(B3LYP)/cc-pVTZ level. <sup>b</sup>  $\Delta E_{el}$  difference of electronic energies ( $E_{hydroxy} - E_{oxo}$ ) calculated at the QCISD/cc-pVDZ or QCISD(T)/cc-pVDZ (given in parentheses) levels at geometry optimized using the DFT(B3LYP)/cc-pVTZ method. <sup>c</sup>  $\Delta F = \Delta G$  difference of free Helmholtz = free Gibbs energies ( $F_{hydroxy} - F_{oxo}$ ) calculated using the  $\Delta E_{el}$  values and thermal and entropy corrections obtained on the basis of the DFT(B3LYP)/cc-pVTZ computed vibrational frequencies and rotational constants.

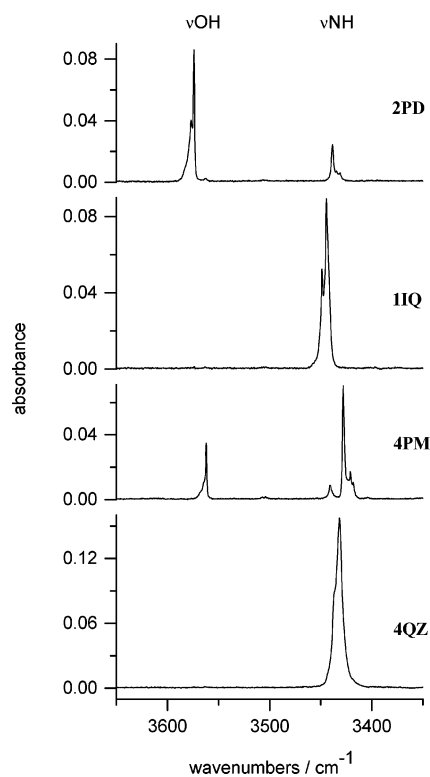
populations of the **2QLh** and **2QLo** tautomers of 2-quinolinone in the matrix (1:95) and to experimentally estimate the  $\Delta F$  for this compound. These values are presented in Table 3, where they are compared with the corresponding data obtained for 2-pyridinone (**2PD**), a single-ring analogue of **2QL**. From this comparison (as well as from the graphical comparison of the high-frequency regions of the IR spectra of **2PD** and **2QL**, presented in Figure 1), it is evident that direct attachment of a benzene ring to the C(5)–C(6) bond of the **2PD** ring leads to a dramatic shift of the tautomeric equilibrium in favor of the higher stability of the oxo tautomer. The experimental observations of tautomeric equilibrium in **2QL** (well supported by the results of theoretical calculations) sharply contradict the previous report by Beak,<sup>4</sup> where the energy difference between **2QLh** and **2QLo** was (unfortunately erroneously) estimated to be -1.2 kJ mol<sup>-1</sup>, in favor of the hydroxy form.

At this point, mentioning the pair of compounds 2-thiopyridine and 2-thioquinoline (analogous to **2PD** and **2QL**, but with sulfur atom replacing oxygen atom) seems also to be noteworthy. Whereas for 2-thiopyridine<sup>35</sup> the thiol form dominates strongly (with the thiol:thione ratio in an Ar matrix equal to 27:1), for 2-thioquinoline<sup>36</sup> the thione form was found to be significantly more stable and the thiol:thione ratio was estimated in this latter case to be equal to 1:7.7. This shows that attachment of a benzene ring considerably shifts the tautomeric equilibrium not only for the oxo compounds (with structure similar to **2PD**), but also for the corresponding thione compounds. Provided that one can treat a thiol tautomer as an analogue of a hydroxy form and a thione tautomer as an analogue of an oxo form, one can say that for both thione and oxo compounds the direction of a change in tautomeric equilibrium, between the “parent” compounds and benzo-annulated derivatives, is the same. For species such as 2-quinoxalinone, 2-quinolinone, and 2-thioquinoline, the stabilities of the oxo or thione tautomers (with respect to

the hydroxy or thiol forms) are significantly higher than those for the single-ring compounds 2-pyridinone, 2-pyrazinone, and 2-thiopyridine.

1-Isoquinolinone (**1IQ**) is an isomer of 2-quinolinone (**2QL**). Although both compounds (**1IQ** and **2QL**) have the same structural elements, **2PD** and a directly fused benzene ring (Chart 1), they differ by the position at which the benzene ring is attached to **2PD**. For **2QL**, the benzene ring is fused at the C(5)–C(6) bond of **2PD** (which is formally a double bond in the structure of the **2PD<sub>o</sub>** form). In the case of **1IQ**, the benzene ring is attached at the C(3)–C(4) bond (double in the **2PD<sub>o</sub>** structure). Quite analogous is the position of a fused benzene ring in the structure of 4-quinazolinone (**4QZ**), for which 4-pyrimidinone (**4PM**) is a “parent”, single-ring compound (Chart 1). Using as a criterion the position of the benzene ring, with respect to the N–C–O fragment, **1IQ** and **4QZ** can be considered as a group of compounds structurally different from **2QX** and **2QL**, discussed in previous paragraphs.

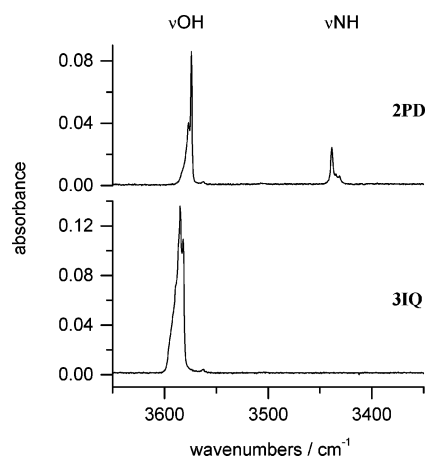
Theoretical calculations, carried out at QCISD and QCISD(T) levels, predict (for **1IQ** as well as for **4QZ**) that tautomeric forms of these compounds should differ in energy by more than 20 kJ mol<sup>-1</sup> (Table 4). For both compounds, the oxo form was predicted to be the significantly more stable tautomer. Free energy differences as big as those calculated for **1IQ** and for **4QZ** should preclude experimental observation of the less stable tautomers. Indeed, in the experimental investigations on **1IQ** and **4QZ** isolated in low-temperature Ar matrixes, no IR bands which could indicate the presence of any amounts of the hydroxy forms were detected. This is illustrated in Figure 3, where at the usual spectral position of a  $\nu(\text{OH})$  band no absorption is visible. Hence, on the basis of experimental and theoretical data, one can conclude that attachment of a benzene ring at a position such as in **1IQ** and **4QZ** leads to very pronounced (even more pronounced than was the case for **2QL** and **2QX**) relative



**Figure 3.** High-frequency regions of the infrared spectra of 2-pyridinone (**2PD**), 1-isoquinolinone (**1IQ**), 4-pyrimidinone (**4PM**), and 4-quinazolinone (**4QZ**) isolated in Ar matrixes. The IR bands present in this spectral range are due to  $\nu(\text{OH})$  and  $\nu(\text{NH})$  vibrations and are characteristic of the hydroxy and oxo tautomers, respectively.

stabilization of oxo tautomeric forms. Although for the “parent”, single-ring compounds (**2PD** and **4PM**) the hydroxy tautomers are well populated, the populations of the hydroxy forms of **1IQ** and **4QZ** in the gas phase must be so low that no traces of these tautomers could be found for **1IQ** and **4QZ** trapped from the gas into low-temperature matrixes.

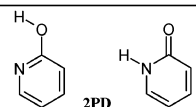
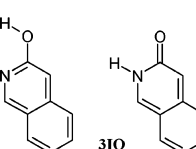
The tautomeric ratios measured for **2QX**, **2QL**, **1IQ**, and **4QZ** strongly suggest that direct attachment of benzene ring at one of the double bonds in the structure of **2PD**, **2PZ**, or **4PM** leads (in a systematic manner) to a significant increase of stability of the oxo tautomers (**2QX**, **2QL**, **1IQ**, and **4QZ**),



**Figure 4.** High-frequency regions of the infrared spectra of 2-pyridinone (**2PD**) and 3-isoquinolinone (**3IQ**) isolated in Ar matrixes. The IR bands present in this spectral range are due to  $\nu(\text{OH})$  and  $\nu(\text{NH})$  vibrations and are characteristic of the hydroxy and oxo tautomers, respectively.

with respect to the corresponding hydroxy forms (**2QXh**, **2QLh**, **1IQh**, and **4QZh**). In an attempt to rationalize these observations, aromaticity of the tautomeric forms of **2PD**, **2PZ**, or **4PM** and their double-ring analogues can be considered. It is obvious that the ring of the hydroxy **2PDh** form is more aromatic than the ring of the oxo **2PD** form; the same is true for analogous pairs of tautomers in **2PZ** and **4PM**. Certainly, higher aromatic character of the **2PDh** ring contributes to the stability of this form much more strongly than is the case for the **2PD** form. The “least aromatic” fragment of the ring of **2PD** (or **2PZ**, or **4PM**) is the N–C bond in the H–N–C=O group. This N–C bond has a single-bond character, which breaks the alternation of single and double bonds around the ring, and hence leads to decrease of its aromaticity. Direct attachment of a benzene ring substantially extends the  $\pi$ -electron system of a molecule. Numerous  $\pi$ -electrons in **2QX**, **2QL**, **1IQ**, and **4QZ** can be shared all over the molecule, making also the heterocyclic rings of the oxo forms somewhat more aromatic. Hence, the single N–C bond in the H–N–C=O group should gain (in **2QX**, **2QL**, **1IQ**, and **4QZ**) a bit of a double-bond character. The results of geometry optimizations carried out for single-ring (**2PD**, **2PZ**, and **4PM**) as well as double-

**TABLE 5: Experimental and Theoretically Calculated Free Energy Differences between the Hydroxy and Oxo Tautomers of 2-Pyridinone and 3-Hydroxyisoquinoline**

compounds	R(C-N) <sup>a</sup>	$\Delta E_{\text{el}}^b$	$\Delta F = \Delta G^c$ at T	$\Delta F_{\text{exp}} = \Delta G_{\text{exp}}$ at T	T	Experimental ratio of hydroxy and oxo forms (at T)
	Å	$\text{kJ mol}^{-1}$	$\text{kJ mol}^{-1}$	$\text{kJ mol}^{-1}$	Kelvin	[hydroxy]:[oxo]
 <b>2PD</b>	1.408	-2.50 (-4.79)	-2.62 (-4.91)	$-2.9 \pm 0.5$	340	2.8 : 1
 <b>3IQ</b>	1.427	-29.54 (-29.00)	-29.34 (-28.80)	< -17	420	oxo form not observed

<sup>a</sup> Distance between C and N atoms in the H–N–C=O fragment of the oxo tautomer. The value has been obtained by geometry optimization carried out at the DFT(B3LYP)/cc-pVTZ level. <sup>b</sup>  $\Delta E_{\text{el}}$  difference of electronic energies ( $E_{\text{hydroxy}} - E_{\text{oxo}}$ ) calculated at the QCISD/cc-pVDZ or QCISD(T)/cc-pVDZ (given in parentheses) levels at geometry optimized using the DFT(B3LYP)/cc-pVTZ method. <sup>c</sup>  $\Delta F = \Delta G$  difference of free Helmholtz = free Gibbs energies ( $F_{\text{hydroxy}} - F_{\text{oxo}}$ ) calculated using the  $\Delta E_{\text{el}}$  values and thermal and entropy corrections obtained on the basis of the DFT(B3LYP)/cc-pVTZ computed vibrational frequencies and rotational constants.

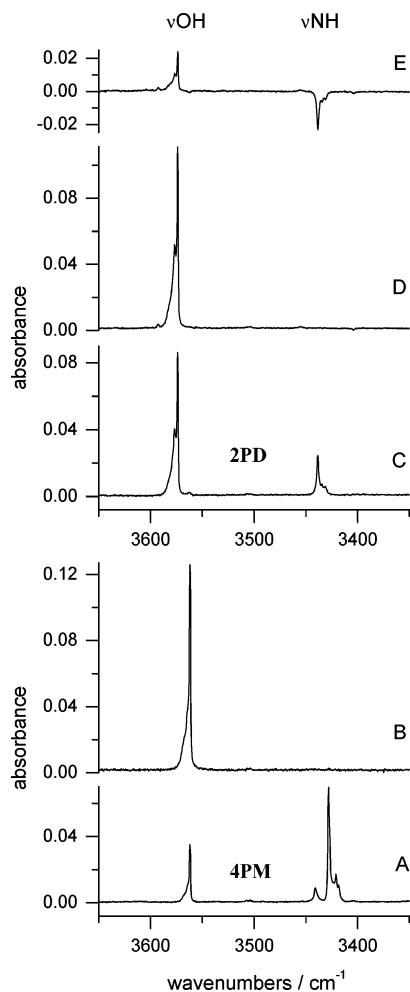


**Figure 5.** High-frequency region of the infrared spectrum of 4-pyrimidinone (**4PM**) isolated in an Ar matrix: (A) spectrum recorded after deposition of the matrix and (B) spectrum recorded after 2 h of UV ( $\lambda > 300$  nm) irradiation. The same region of the infrared spectrum of 2-pyridinone (**2PD**) isolated in an Ar matrix: (C) spectrum recorded after deposition of the matrix, (D) spectrum recorded after 1 h of UV ( $\lambda > 300$  nm) irradiation, and (E) difference spectrum, trace D minus trace C.

ring (**2QXo**, **2QLo**, **1IQo**, and **4QZo**) compounds show that, with the attachment of a benzene ring, the N–C bond (in H–N–C=O) gets systematically shorter (Tables 3 and 4). This suggests that the difference of aromaticity of the heterocyclic rings of the hydroxy and oxo tautomers is somewhat reduced in double-ring compounds, in comparison to their single-ring analogues. Therefore, the stability advantage of the hydroxy forms, introduced by the aromaticity factor, should be much lower for double-ring systems than it was for single-ring species. By such considerations, the simplest possible system of oxo and hydroxy forms of formamide has to be taken as a reference. For this compound, the aromaticity factors (in a sense discussed above) do not exist at all. As it results from experimental observations<sup>37,38</sup> and theoretical calculations,<sup>14</sup> the oxo tautomer of formamide is more stable (by at least 40 kJ mol<sup>-1</sup>) than the hydroxy form of this compound. In 2-pyridinone the higher stability of the oxo form of the amide group is balanced by the higher stability of the aromatic ring in the hydroxy form. For **2QX**, **2QL**, **1IQ**, and **4QZ**, where the aromaticity advantage of the hydroxy tautomers is noticeably reduced, the oxo tautomeric forms become again the most stable.

**3-Hydroxyisoquinoline.** Alongside **2QL** and **1IQ**, which are two compounds built of benzene and **2PD** subunits fused

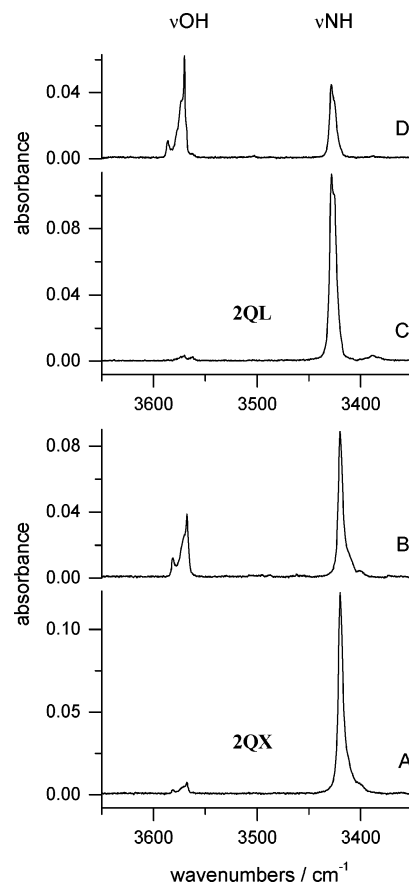


**Figure 6.** High-frequency region of the infrared spectrum of 2-quinoxalinone (**2QX**) isolated in an Ar matrix: (A) spectrum recorded after deposition of the matrix and (B) spectrum recorded after 6.5 h of UV ( $\lambda > 335$  nm) irradiation. The same region of the infrared spectrum of 2-quinolinone (**2QL**) isolated in an Ar matrix: (C) spectrum recorded after deposition of the matrix and (D) spectrum recorded after 4.5 h of UV ( $\lambda > 320$  nm) irradiation.

together, there exists also a third isomer, 3-hydroxyisoquinoline (**3IQ**). This latter compound **3IQ** is built by a fusion of the two rings at the C(4)–C(5) bond of **2PD** (Chart 1). However, it does not seem that **3IQ** is just a third isomer, which should be similar in its properties to **2QL** and **1IQ**. The very fact that in **2QL** and **1IQ** benzene is attached at one of the double bonds of the **2PD**o form, whereas in **3IQ** the two rings are fused at the C(4)–C(5) bond of **2PD** (formally single in **2PD**o), turned out to be of crucial importance for stabilization of the **3IQ**o tautomer. For the hydroxy form of **3IQ**, the single- and double-bond system in both rings is regularly aromatic, but the single- and double-bond system in the oxo **3IQ**o tautomer does not contribute well to the stabilization of this form. This destabilization is reflected in the results of theoretical prediction of relative energies of the **3IQh** and **3IQo** tautomers. The energy of **3IQh** was calculated at both QCISD and QCISD(T) levels to be lower by 29 kJ mol<sup>-1</sup> than the energy of the **3IQo** form (Table 5). The experimental observations on **3IQ** monomers isolated in an Ar matrix are in full agreement with the theoretical predictions. Only the hydroxy **3IQh** form was experimentally observed, with the **3IQo** population (if any) below the detection limits. This is reflected in the high-frequency region of the infrared spectrum of **3IQ** (Figure 4), where only the  $\nu(\text{OH})$  band is observed and no absorption is detectable at the usual position of the  $\nu(\text{NH})$  band.

**Phototautomeric Oxo  $\rightarrow$  Hydroxy Reactions.** UV-induced processes, leading to the proton shift from NH group to the oxygen atom of the adjacent carbonyl group, were previously



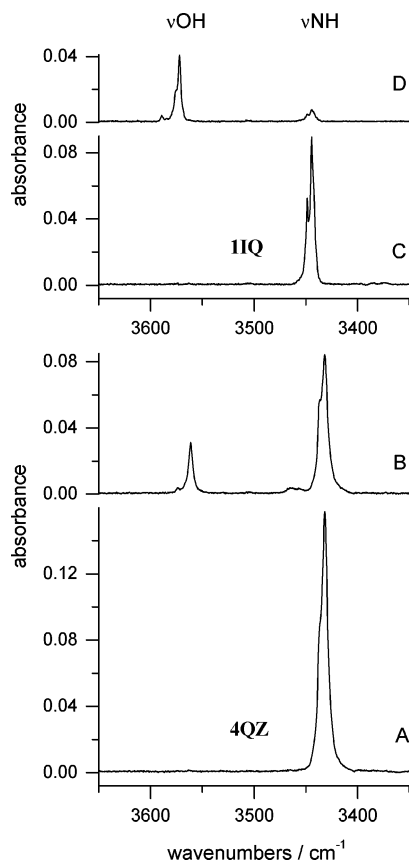
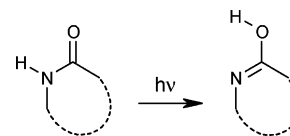


**Figure 7.** High-frequency region of the infrared spectrum of 4-quinazolinone (**4QZ**) isolated in an Ar matrix: (A) spectrum recorded after deposition of the matrix and (B) spectrum recorded after 4.5 h of UV ( $\lambda > 300$  nm) irradiation. The same region of the infrared spectrum of 1-isoquinolinone (**1IQ**) isolated in an Ar matrix: (C) spectrum recorded after deposition of the matrix and (D) spectrum recorded after 1.5 h of UV ( $\lambda > 320$  nm) irradiation.

observed for several matrix-isolated molecules containing the amide  $\text{—NH—CO—}$  moiety (Scheme 1). Such photochemical processes transform the oxo tautomeric forms of simple amides<sup>37–39</sup> or heterocyclic amides<sup>9,19,20,22,40</sup> into the corresponding hydroxy tautomers. The phototautomeric reactions, occurring for single-ring compounds 2-pyridinone<sup>9</sup> and 4-pyrimidinone<sup>19,20,22</sup> isolated in low-temperature matrixes, are illustrated in Figure 5. In this figure the changes in intensities

### SCHEME 1: Unimolecular Oxo–Hydroxy Photoreaction in Simple and Heterocyclic Amides



of the bands due to  $\nu(\text{OH})$  and  $\nu(\text{NH})$  stretching vibrations represent changes of populations of the hydroxy and oxo tautomers. For 2-pyridinone and 4-pyrimidinone, it was possible (by using filtered UV radiation) to convert almost all molecules (initially present in the matrix in the oxo form) into the hydroxy tautomer. The choice of an appropriate cutoff filter was guided by the fact that the oxo tautomeric forms of the compounds in question absorb at longer wavelengths than their hydroxy counterparts. The energies of 0–0 electronic transitions were previously determined by dispersed fluorescence and fluorescence excitation spectra, for 2-pyridinone, 4-pyrimidinone, and 2-quinolinone tautomers in supersonic jet expansions. The 0–0 lines in these spectra were found at 335 and 277 nm for **2PDo** and **2PDh**,<sup>41</sup> at 328 and 283 nm for **4PMo** and **4PMh**,<sup>42</sup> and at 344 and 319 nm for **2QLo** and **2QLh**,<sup>5</sup> respectively. If the wavelength of the UV light used for irradiation of a matrix was such that only the oxo form was excited, then only the oxo  $\rightarrow$  hydroxy transformation was induced and complete transformation of all the molecules into the hydroxy form was observed. In a dedicated experiment (carried out for **4PM**),<sup>43</sup> the first irradiation of the matrix (leading to total conversion of all the material to the hydroxy form) was followed by an irradiation with shorter wavelength UV light ( $\lambda > 230$  nm). This led to partial recovery of the population of the oxo form (totally consumed during the first irradiation). Hence, the occurrence of the photoreaction in the hydroxy  $\rightarrow$  oxo direction (accompanying the dominating oxo  $\rightarrow$  hydroxy phototransformation) was demonstrated and the photoreversibility of the phototautomeric reaction was proven.

On the basis of the fragments of spectra of **2QX**, **2QL**, **1IQ**, and **4QZ**, recorded before and after UV irradiation of the matrixes (Figures 6 and 7), one can conclude that the oxo  $\rightarrow$  hydroxy phototautomeric reaction occurs also for monomers of these bicyclic heterocycles. This photoreaction converts the oxo forms (**2QXo**, **2QLo**, **1IQo**, and **4QZo**) into the hydroxy tautomers (**2QXh**, **2QLh**, **1IQh**, and **4QZh**, respectively). The spectra presented in Figures 6 and 7 suggest that for **2QX**, **2QL**,

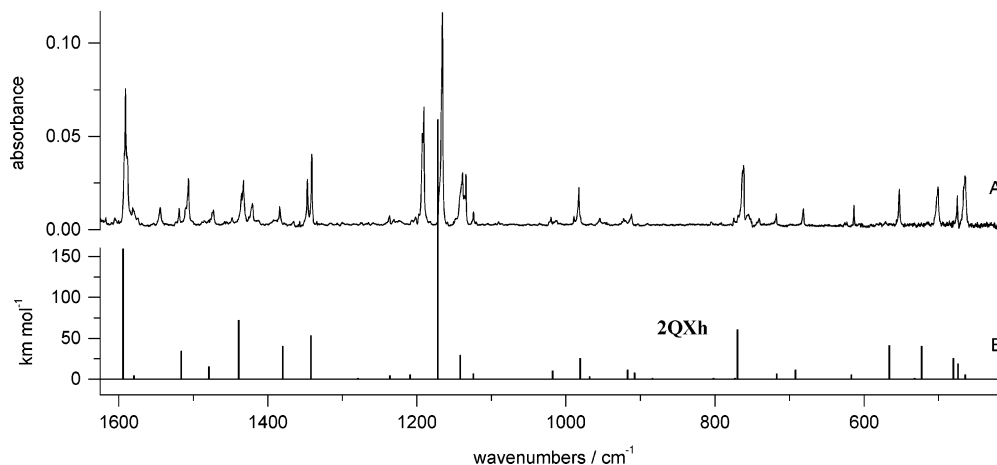


**Figure 8.** (A) Infrared spectrum of the photoproduct generated upon 6.5 h of UV ( $\lambda > 335$  nm) irradiation of 2-quinoxalinone isolated in an Ar matrix. The spectrum of the unreacted substrate of the photoreaction (the oxo tautomer **2QXo**) has been removed by electronic subtraction. (B) Infrared spectrum of the hydroxy tautomer **2QXh** theoretically predicted at the DFT(B3LYP)/cc-pVTZ level. The calculated wavenumbers were scaled by the single factor of 0.98.

**1IQ**, and **4QZ** the oxo form cannot be totally and quantitatively phototransformed into the hydroxy form. There are two possible reasons for that. First, due to photoreversibility of the photo-tautomeric reaction, the final stage of the simultaneous oxo  $\rightarrow$  hydroxy and hydroxy  $\rightarrow$  oxo processes can be a photostationary state. Second, the phototautomeric reactions in **2QL**, **1IQ**, and **4QZ** were accompanied (to a greater or lesser extent, depending on the compound and wavelengths of the applied UV light) by competing photoreaction(s), partially consuming the reagent. As a rule, the progress of the phototautomeric reactions in **2QX**, **2QL**, **1IQ**, and **4QZ** was considerably slower than was the case for single-ring compounds **2PD** and **4PM**. Although it was quite slow, the photoreaction induced by UV irradiation of the oxo **2QXo** form of 2-quinoxaline seems to produce only one product: the hydroxy **2QXh** tautomer. This is illustrated (Figure 8) by a good agreement between the experimental IR spectrum growing in the course of UV irradiation (the spectrum of the photoproduct species) with the spectrum calculated at the DFT-(B3LYP) level for the **2QXh** form.

## Conclusions

The systematic survey of tautomerism of benzo-annelated derivatives of 2-pyridinone, 4-pyrimidinone, and 2-pyrazinone revealed a substantial influence of fusion with a benzene ring on the oxo-hydroxy equilibrium. It was shown, using experimental and theoretical methods, that (except for a special case of 3-hydroxyisoquinoline) benzo-annelation leads to significant stabilization of the oxo tautomers with respect to the hydroxy forms. This effect was demonstrated for 2-quinolinone, 1-isoquinolinone, 2-quinoxalinone, and 4-quinazolinone. A similar shift of a tautomeric equilibrium has recently been theoretically predicted for cytosine and its benzo-fused derivative.<sup>44</sup> It seems probable that an effect of the same nature contributes to greater stabilization of the oxo forms (relative to the hydroxy tautomers) of hypoxanthine and allopurinol,<sup>43,45</sup> with respect to a corresponding tautomeric equilibrium in 4-pyrimidinone. In all of these cases, extension of a  $\pi$ -electron system (being a consequence of direct attachment of a second ring) seems to be the crucial factor. The results described in the present paper should contribute to better understanding of a link between aromaticity and tautomerism.<sup>46</sup>

**Acknowledgment.** This study was partially supported by NSF CREST Grant 9805465.

## References and Notes

- Löwdin, P.-O. *Adv. Quantum Chem.* **1965**, 2, 213.
- Pullman, B.; Pullman, A. *Adv. Heterocycl. Chem.* **1971**, 13, 77.
- Topal, M. D.; Fresco, J. R. *Nature* **1976**, 263, 285.
- Beak, P. *Acc. Chem. Res.* **1977**, 10, 186.
- Nimlos, M. R.; Kelley, D. F.; Bernstein, E. R. *J. Phys. Chem.* **1987**, 91, 6610.
- Held, A.; Plusquellic, D. F.; Tomer, J. L.; Patt, D. W. *J. Phys. Chem.* **1991**, 95, 2877.
- Fabian, W. M. F.; Niederreiter, K. S.; Uray, G.; Stadlbauer, W. *J. Mol. Struct.* **1999**, 477, 209.
- Hatherley, L. D.; Brown, R. D.; Godfrey, P. D.; Pierlot, A. P.; Caminati, W.; Damiani, D.; Melandri, S.; Favero, L. B. *J. Phys. Chem.* **1993**, 97, 46.
- Nowak, M. J.; Lapinski, L.; Fulara, J.; Les, A.; Adamowicz, L. *J. Phys. Chem.* **1992**, 96, 1562.
- Parchment, O. G.; Burton, N. A.; Hillier, I. H. *Chem. Phys. Lett.* **1993**, 203, 46.
- Dkhissi, A.; Houben, L.; Smets, J.; Adamowicz, L.; Maes, G. *J. Mol. Struct.* **1999**, 484, 215.
- Wong, M. W.; Wiberg, K. B.; Frisch, M. J. *J. Am. Chem. Soc.* **1992**, 114, 1645.
- Moreno, M.; Miller, W. *Chem. Phys. Lett.* **1990**, 171, 475.
- Piacenza, M.; Grimme, S. *J. Comput. Chem.* **2004**, 25, 83.
- Lochbrunner, S.; Wurzer, A. J.; Riedle, E. *J. Chem. Phys.* **2000**, 112, 10699.
- Lochbrunner, S.; Stock, K.; Riedle, E. *J. Mol. Struct.* **2004**, 700, 13.
- Nagaoka, S.; Kusunoki, J.; Fujibuchi, T.; Hatakenaka, S.; Mukai, K.; Nagashima, U. *J. Photochem. Photobiol., A* **1999**, 122, 151.
- Guallar, V.; Batista, V. S.; Miller, W. H. *J. Chem. Phys.* **2000**, 113, 9510.
- Nowak, M. J.; Lapinski, L.; Fulara, J. *J. Mol. Struct.* **1988**, 175, 91.
- Lapinski, L.; Fulara, J.; Nowak, M. J. *Spectrochim. Acta, Part A* **1990**, 46, 61.
- Lapinski, L.; Nowak, M. J.; Les, A.; Adamowicz, L. *Vibr. Spectrosc.* **1995**, 8, 331.
- Lapinski, L.; Nowak, M. J.; Les, A.; Adamowicz, L. *J. Am. Chem. Soc.* **1994**, 116, 1461.
- Karmas, G.; Spoeri, P. *J. Am. Chem. Soc.* **1952**, 74, 1580.
- Kanakahara, T.; Takagi, Y. *Heterocycles* **1978**, 9, 1733.
- Jones, R. G. *J. Am. Chem. Soc.* **1949**, 71, 78.
- Becke, A. *Phys. Rev. A* **1988**, 38, 3098.
- Lee, C. T.; Yang, W. T.; Parr, R. G. *Phys. Rev. B* **1988**, 37, 785.
- Vosko, S. H.; Wilk, L.; Nusair, M. *Can. J. Phys.* **1980**, 58, 1200.
- Woon, D. E.; Dunning, T. H., Jr. *J. Chem. Phys.* **1993**, 98, 1358.
- Pople, J. A.; Head-Gordon, M.; Raghavachari, K. *J. Chem. Phys.* **1987**, 87, 5968.
- Møller, C.; Plesset, M. S. *Phys. Rev.* **1934**, 46, 618.
- Salter, E. A.; Trucks, G. W.; Bartlett, R. J. *J. Chem. Phys.* **1989**, 90, 1752.
- Gauss, J.; Stanton, J. F.; Bartlett, R. J. *J. Chem. Phys.* **1991**, 95, 2623.
- Frisch, M. J.; Trucks, G. W.; Schlegel, H. B.; Scuseria, G. E.; Robb, M. A.; Cheeseman, J. R.; Montgomery, J. A., Jr.; Vreven, T.; Kudin, K. N.; Burant, J. C.; Millam, J. M.; Iyengar, S. S.; Tomasi, J.; Barone, V.; Mennucci, B.; Cossi, M.; Scalmani, G.; Rega, N.; Petersson, G. A.; Nakatsuji, H.; Hada, M.; Ehara, M.; Toyota, K.; Fukuda, R.; Hasegawa, J.; Ishida, M.; Nakajima, T.; Honda, Y.; Kitao, O.; Nakai, H.; Klene, M.; Li, X.; Knox, J. E.; Hratchian, H. P.; Cross, J. B.; Bakken, V.; Adamo, C.; Jaramillo, J.; Gomperts, R.; Stratmann, R. E.; Yazyev, O.; Austin, A. J.; Cammi, R.; Pomelli, C.; Ochterski, J. W.; Ayala, P. Y.; Morokuma, K.; Voth, G. A.; Salvador, P.; Dannenberg, J. J.; Zakrzewski, V. G.; Dapprich, S.; Daniels, A. D.; Strain, M. C.; Farkas, O.; Malick, D. K.; Rabuck, A. D.; Raghavachari, K.; Foresman, J. B.; Ortiz, J. V.; Cui, Q.; Baboul, A. G.; Clifford, S.; Cioslowski, J.; Stefanov, B. B.; Liu, G.; Liashenko, A.; Piskorz, P.; Komaromi, I.; Martin, R. L.; Fox, D. J.; Keith, T.; Al-Laham, M. A.; Peng, C. Y.; Nanayakkara, A.; Challacombe, M.; Gill, P. M. W.; Johnson, B.; Chen, W.; Wong, M. W.; Gonzalez, C.; Pople, J. A. *Gaussian 03*, revision C.02; Gaussian, Inc.: Wallingford, CT, 2004.
- Nowak, M. J.; Lapinski, L.; Rostkowska, H.; Les, A.; Adamowicz, L. *J. Phys. Chem.* **1990**, 94, 7406.
- Prusinowska, D.; Lapinski, L.; Nowak, M. J.; Adamowicz, L. *Spectrochim. Acta, Part A* **1995**, 51, 1809.
- Maier, G.; Endres, J. *Eur. J. Org. Chem.* **2000**, 1061.
- Duvernay, F.; Trivella, A.; Borget, F.; Coussan, S.; Aycard, J. P.; Chiavassa, T. *J. Phys. Chem. A* **2005**, 109, 11155.
- Duvernay, F.; Chiavassa, T.; Borget, F.; Aycard, J. P. *J. Phys. Chem. A* **2005**, 109, 6008.
- Lapinski, L.; Fulara, J.; Czerminski, R.; Nowak, M. J. *Spectrochim. Acta, Part A* **1990**, 46, 1087.
- Nimlos, M. R.; Kelley, D. F.; Bernstein, E. R. *J. Phys. Chem.* **1989**, 93, 643.
- Tsuchiya, Y.; Tamura, T.; Fujii, M.; Ito, M. *J. Phys. Chem.* **1988**, 92, 1760.
- Gerega, A.; Lapinski, L.; Reva, I.; Rostkowska, H.; Nowak, M. J. *Biophys. Chem.* **2006**, 122, 123.
- Huertas, O.; Blas, J. R.; Soteras, I.; Orozco, M.; Luque, F. J. *J. Phys. Chem. A* **2006**, 110, 510.
- Gerega, A.; Lapinski, L.; Nowak, M. J.; Rostkowska, H. *J. Phys. Chem. A* **2006**, 110, 10236.
- Balaban, A. T.; Oniciu, D. C.; Katritzky, A. R. *Chem. Rev.* **2004**, 104, 2777.